International Journal of Hybrid Innovation Technologies
Vol.1, No.1 (2021), pp.69-82
http://dx.doi.org/10.21742/ijhit.2021.1.1.06

Automatic Lung Field Segmentation using Robust Deep Learning Criteria

Mohammed Ryiad Al-Eiadeh

Al Yarmouk University, Jordan
mohammed.r.eiadeh@gmail.com

Abstract

The chest X-Ray image is one of the common image types that describe medical imaging for medical purposes, its more common than other medical image types like MRI, CT scan, and PET scan. Huge medical tests that depend on the CXR-images are difficult to deal with X-Ray images on both radiologists and medical practitioners. the organ partitioning is a step to obtain an efficient computer-aided detection and how the computer vision can be used to provide good functionality in medical aided diagnosis systems depending on the deep learning. Lung field segmentation plays an important role in medical diagnosis systems like a task to classify whether the image belongs to a normal or abnormal person based on the shape of the segmented or predicted lung field. We proposed a model that combined the DeepLabv3 plus with ResNet-18 to build a segmentation network that performs decoding and encoding phases to extract the spatial features of a particular area and output the segmented one, respectively. The model is evaluated on a public dataset Montgomery County set - Chest X-ray Database, multiple experiments were conducted by dividing the data into 60% for training and the rest 40% for testing, the experiment was repeated 10 times as for each time data divisors were randomly selected to support our model performance. Our model Performance measurements achieved Dice=96.9 % and Jaccard=94.1% which shown the robustness of our proposed approach.

Keywords: *Automatic lung field segmentation, Semantic segmentation, Instance segmentation, Deeplabv3plusLayers, Segmentation network, Encoder-decoder architecture*

1. Introduction

Since it's known that the medical field is the most critical because it specializes in human being health risk, disease diagnosis, and many others, then it's very important to deal with the previously mentioned critical processes with very high precision and fast well. Building many computational models that automatically give decisions and predictions for a human being health risk [1], clinical decision support [2], and many other important functions. Where such these models used many resources such that human knowledge, data like images and texts, probabilities, etc. [3]. It is worth mentioning that life has many important sectors, but the human health care sector is on a high level of priority over the other ones.

Early, the medical expert systems have covered a huge number of tasks that depend on medical data like images. These systems are also become too widely of usage because of the success due to deep learning. Since a lot of these expert systems used images to perform and

Article history:
Received (February 10, 2021), Review Result (April 4, 2021), Accepted (August 1, 2021)

eISSN: 2653-309X IJHIT

achieve a lot of medical tasks in high performance. The structure of images has multi-object even in the same image. Images are used in many medical purposes and tasks like diagnosis, classification, etc. [4]. Some tasks may need only a specific area from the image and this is image segmentation (extract a particular number of pixels or dividing, and partitioning image into parts) [5].

Image segmentation plays an active role in a huge number of medical systems in various ways such that automating or facilitating the delineation of anatomical structures and, other regions of interest [6]. The inputs of the medical systems are various like X-ray images [7]. The subject of this study is the lung field segmentation from chest CXR images. The lung field segmentation task is one of the strong challenges that face Computer Scientists, because of the obstacles they are going to face when trying to build a lung field segmentation system.

Since X-ray images are unclear (contains parts that weaken the resolution of the interesting area), and the Lung field shape is different from one person to another. The input data of this study are CXR images that had been taken by human experts from many patients and fed to a robust deep learning system. There are a lot of various image segmentation systems, whereas some of the most popular are thresholding methods, edge detection-based techniques, region-based techniques, clustering-based techniques, watershed-based techniques, partial differential equation-based techniques, and artificial neural network-based techniques [5][8]. Many researchers have been involved in this task by building several models depending on their thoughts, we are going to talk about some of them in the literature review section attempting to talk about each one of them to show the differences between them. Some studies had used deep learning neural networks because it's very strong learners with some optimization algorithms, and some of them consist of pre-processes and post-processes to enhance the achieved results, whereas others used some different criteria based on some statistical approaches [9].

2. Literature review

This section provides an overview of several proposed studies that had been conducted to develop various lung field segmentation systems to detect lung field disease through lung X-ray images. Moreover, this section summarizes several proposed methodologies by recent studies on this problem and documents the general pipeline of their works.

Dai et al. [8] proposed a system that combined two fully convolutional networks that are critic network and the segmentation network for training and testing processes respectively. Their system called Structure Correction Adversarial Network (SCAN) is employed to segment two parts of the lung (heart and fields). SCAN can train without an existing dataset and can be used on CXR images for various populations.

Li et al. [9] proposed a system that depends on a statistical shape and appearance model. Features were extracted from the image by distributed points referred to the shape of an object and stored in a vector of features. The features of the test images were extracted and compared with the training ones to find the similarity and dissimilarity measurements to determine the position of the targeted objects.

Stirenko et al. [10] proposed a system used to predict the availability of tuberculosis for computer-aided diagnosis tasks. Their system depends on a deep CNN which was trained on a small and non-well-balanced dataset which may decrease the efficiency of the CNN. They solved the balancing issue by performing some data augmentation techniques. Hassan et al [11] proposed a system that depends on a Fully Convolutional Neural Network (FCNN) which is divided into four steps such that, first step included training the CNN. The rest three steps were used as post processes to improve the segmentation results, where flood fil algorithm was used

to fill some minor holes of some results, removing some unwanted object from the image, and used a morphological opening algorithm to separate the lung fields from some images that were fused merged.

Wang [12] proposed a system to segment different parts of the chest like lung fields, heart, and clavicles. This system depends on a hybrid multi-task Convolutional Network (FCN) with various functions for the segmentation process, where a U-net network is used for the training process. They used the fast level set algorithm to remove the holes of the produced results to improve their model efficiency. FridAdar et al. [13] proposed a system to segment lung fields, heart, and clavicles parts. Their system depends on employing different types of neural networks to train the model with different loss functions for different classes. They acknowledged that the best network from the proposed one was U-net with VGG-16 as decoder and encoder respectively. Zhang et al proposed a system consisted of pre-processes such as cropping, zooming, horizontal flipping, and many others to prepare data for training and testing phases. U-net was used to train the model and some methods were performed to ignore some irrelevant parts of the outputs.

Tang et al. [14] proposed a system consisted of a data augmentation process that was achieved by the image-to-image translation method. on the deep residual neural network called ResNet-101 to segment the lung fields. Solovyev et al [15] proposed a system to segment lung fields and heart parts. Their system employed an altered CNN by obtaining the ResNet-50 backbone and Monti-Carlo dropout.

Yang et al. [16] proposed a system used to detect the lung fields. Their system depends on a high-quality detector called Structured Edge Detector like deep edges which are pre-trained learners. An ultra-metric map used to show edges of the lung structure used to detect the fields and its very fast method because it can process 256 X 256 pixels image by less than a tenth of a second, where it's very accurate with different radiograph units.

Xiong et al. [17] proposed a system consisted of initialization, deformation, and regularization processes. Initialization (voting strategy) was used to vote for the most suitable shape that could be obtained for the input image. The outputs were processed by deformation and regularization to obtain the convergence state of the shape and to improve the efficiency of the model.

Candemir et al. [18] proposed a method called anatomical atlases with nonrigid registration that consisted of three processes that retrieve images based on the training data with their corresponding ground truth masks, used a shift flow method to create the initial lung field shape to be used for training step, and graph cut optimization approach used with a customized energy function to extract the lung boundaries.

According to the previous works, we can conclude that most proposed works for such tasks depend on modern neural networks that can extract spatial information of an object from the image. In this work, we proposed a model consists of three contributions such that: performing data preparation preprocesses to enhance the input data to the model, using modern encoder-decoder neural networks for training and testing processes, and removing the unwanted objects of some results.

3. Methodology

In the methodology section, we try to explain our clue and how we can study the task by using the neural network approach. Supporting our idea with diagrams, figures, and images to make our idea so clear, understandable, and explaining our model with its behavior.

2.1. General overview

The proposed automatic lung field segmentation model briefly divides into several dependent steps. The workflow of our model is performing several pre-processes on the used dataset, using the data to train deeplabv3plusLayer combining with neural network ResNet-18 to create an encoder and decoder architecture [19] to be able to classify the pixels into two classes (foreground and background pixels). Training this model requires two data stores one for the CXR-images and the other one is for the ground truth masks. The testing phase for testing our model to produce the segmentation results, and we performed a post pre-process which is used to remove tiny unwanted objects of some results.

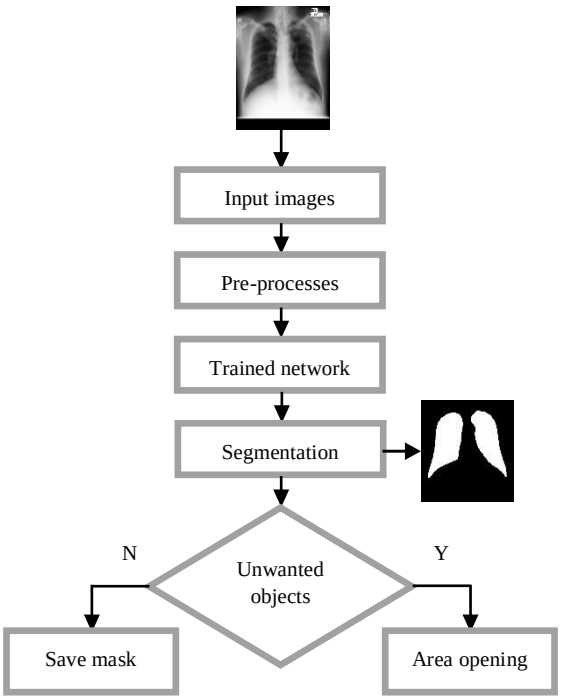

Figure 1. The workflow of the proposed model

2.2. Decoder and encoder architecture

The previous neural networks used few operations such as probing the entering features with some filters or some pooling operations at multiple rates to encode multi-scale contextual information, whilst modern neural- networks are capable to capture sharper object boundaries by progressively retrieving the spatial information. One of the modern neural networks is the DeepLabV3 plus which is an efficient encoder. In this section, we will talk about few topics such that Atrous convolution, Depth wise separable convolution, the encoder, and the decoder.

2.3. Atrous convolutional

Atrous convolution can be used in deep convolutional networks to control the resolution of the computed features and capture multi-scale information by regulating the filter's field of view. A chest X-ray produces black and white images that show the organs of the chest [20]. That type of image is a two-dimensional signal which is a function of spatial coordinates X and Y, then an intensity value is assigned for each point (X, Y) [21]. In tasks like lung field

segmentation, the objects came within various sizes which means feature maps must be able to cover various scales of receptive fields. DeepLabV3 handles that by two strategies that are cascade and parallel with several numbers of Atrous convolutional layers with various dilation rates [22]. ASPP is an abbreviation of Atrous Spatial Pyramid Pooling which referred to parallel mode, the output feature maps are a sampling of the input feature maps with various scales of receptive fields.

Assume that x is an input feature map, y is an output feature map and w is the convolutional filter with the k size and symbol r is the dilation rate then applying Atrous convolutional on x such that for each point that is on x will be computed as:

$$[i] = \sum_{j=1}^{k} X\,[i + r.k].w[k] \quad (1)$$

The Atrous convolution filter is UpSampled by $(r-1)$ inserting zeros between two consecutive filter values in each spatial $(r-1)$ dimension which is the same to insert blanks between each two $r = 1$ consecutive filter values if the convolutional become standard convolution [23].

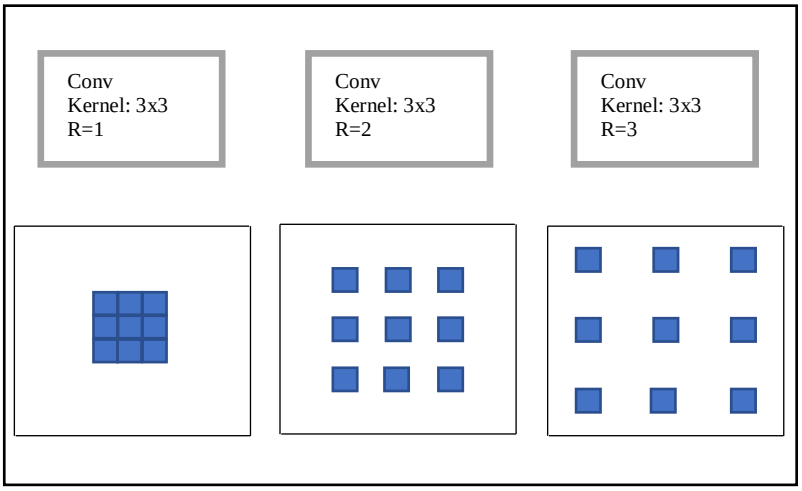

Figure 2. Atrous convolution with = 1,2,3 respectively

The output feature maps are very sensitive to the location of the features in the input feature maps. DownSampling the output feature maps will handle the sensitivity problem, DownSampling is achieved by the pooling layer. Two common pooling layer operations are average and max pooling [24]. The pooling layers will always decrease the size of the dimension of the output feature map by a factor of 2 where the dimension of the output feature map is halved of the previous one and so on. The output feature map will be very small after several pooling operations. Pooling operations are very useful for capturing long-range information, but it is not useful for semantic segmentation tasks since it needs a lot of details of spatial information.

Atrous convolution allows us to capture features at multi scales and keep the spatial resolution as the resolution of the input image, this is done by increasing the dilation rate at each block to expand the field of view of the filter for better semantic segmentation results. Various field of view is creating by setting distinct dilation rates to extract multi contextual information without decreasing the size of the output feature maps.

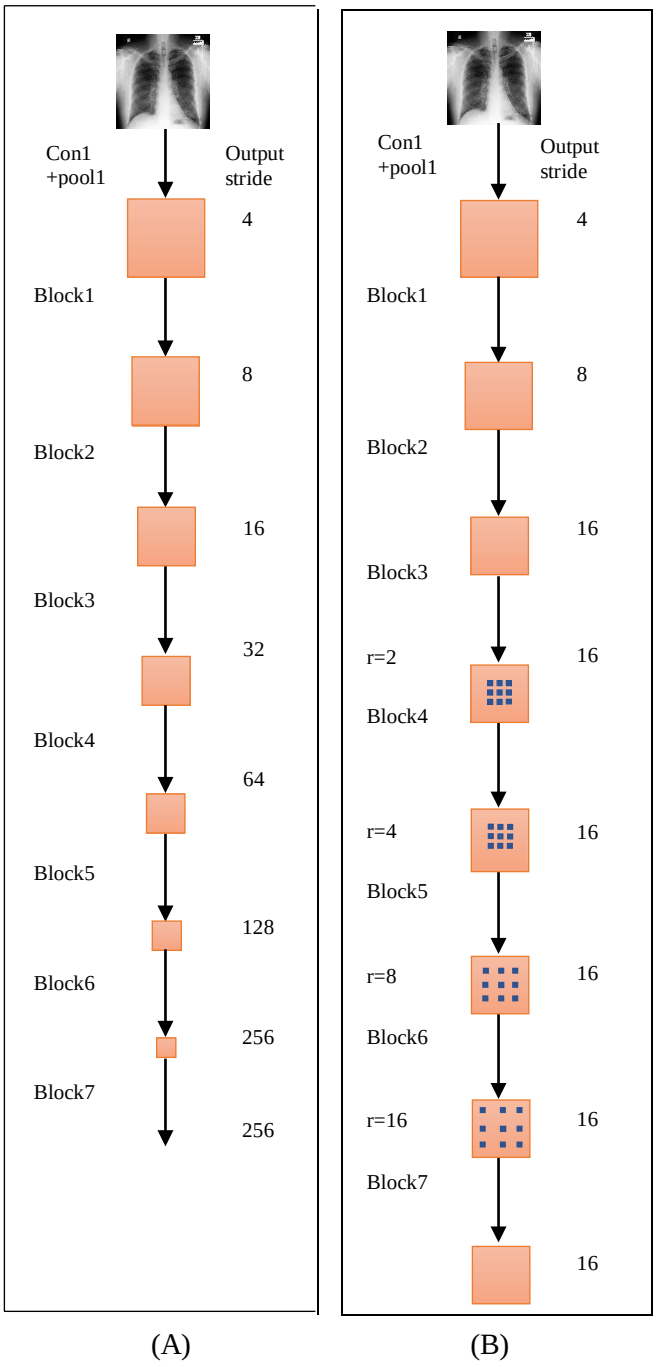

Figure 3. Standard conv on the left and Atrous conv on the right

2.4. DepthWise separable convolutional

Performing Atrous convolutions to extract the spatial information from the input feature maps will take a while which a time consuming, then to reduce that's computation complexity with the same performance we used the DepthWise convolution mechanism. It transfers the standard convolution into a DepthWise convolution followed by a 1x1 convolution. DepthWise convolution decreases the number of the parameters which is used in the convolution layer

operations. An example of an approach that used a DepthWise convolution is Xception which was proposed by google [25].

In DepthWise convolution each input channel in the input feature map will be passed throw a DepthWise convolution to perform a spatial convolution. DepthWise convolution is independently performed for each input channel then the outputs will be combined by the point-wise convolution.

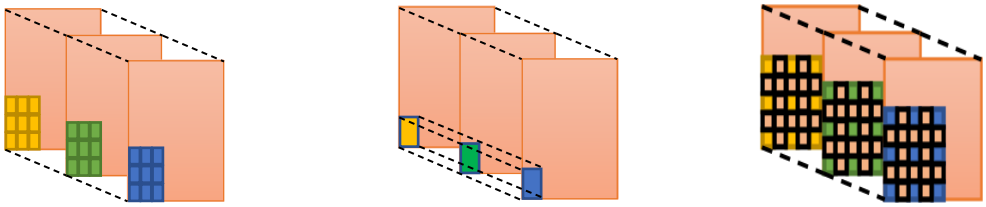

(A) DepthWise conv (B) PointWise conv (C) Atrous DepthWise conv

Figure 4. (A) 3x3 DepthWise separable conv from standard conv into DepthWise conv, (B) pointwise which combines outputs after performing a DepthWise conv on each channel among all channels, and (C) Atrous DepthWise conv on each channel with dilation rate equals to 2

2.5. DeepLabV3 as encoder

The DeepLabV3 used Atrous convolution to extract features computed by the convolution neural network at multi scales and controlled their resolution. Atrous conv supports the DepthWise separable conv for extracting the features in parallel mode to reduce the computation time based on the resources budget. In the image classification tasks, the spatial resolution of the final feature map is usually 32 times smaller than the input image resolution which is that the output strid=32, but in the semantic segmentation tasks the spatial resolution must be very rich information which done by reducing the output stride to be 16 by applying Atrous conv with the dilation rate (r=2) to the last two blocks (the second conv layer at first block and both first and second conv layer at the second block) to get denser feature extraction. By applying ASPP network which has four parallel Atrous convolutions that apply Atrous conv with various dilution rates (r=6, 12, 18) to extract spatial information at different scales (obtain multi-scale contextual information). The outputs of the four Atrous convolutions are combined by the concatenation layer (catAspp) which is a 1x1 convolution.

2.6. ResNet-18 as decoder

In this model, we proposed a very effective decoder-based ResNet-18. The first step is to bilinearly UpSample the extracted features (by the encoder) by a factor of 4. Note that the dec-UpSample2 layer is a transposed convolution layer that has the same connectivity as the normal conv but in the backward direction which can be used to conduct the UpSampled operation on the input features map [26]. In this model we used UpSample2 which doubles the dimension of the input matrix [27], then concatenates the UpSampled output (rich semantic details) with the low-level features used in modern backbone neural networks like ResNet-18. Low-level features have very rich spatial details but lack semantics because it's too noisy to provide high-resolution semantics [28]. handling that lack problem by concatenated the low-level features with the outputs of the UpSampled operation. Since low-level features contain a very large number of channels which may cause the training to become harder. Applying 1 x 1 convolution

to decrease the number of channels (256 channels used in our model). Applying few 3 x 3 convolutions to refine the features, after that applying another bilinearly UpSampled operation by the factor of 4. Softmax and classification layers are the last two layers in the network. The softmax layer applied a softmax function to turn the vector of M real values into a vector of real values that their summation equals 1 to be considered as probabilities [29]. The output of the softmax passes into the classification layer.

The classification layer used to compute the cross-entropy loss function to classify mutually exclusive classes [30], cross-entropy loss function can be formulated as:

$$cross\ entroop = -\sum_{i=1}^{N}\sum_{l=1}^{C} til\ ln\ yil \tag{2}$$

$cross\ entroop$ is the cross-entropy loss, N is the number of samples, C is the number of classes, and til is the indicator that the sample belongs to the class l

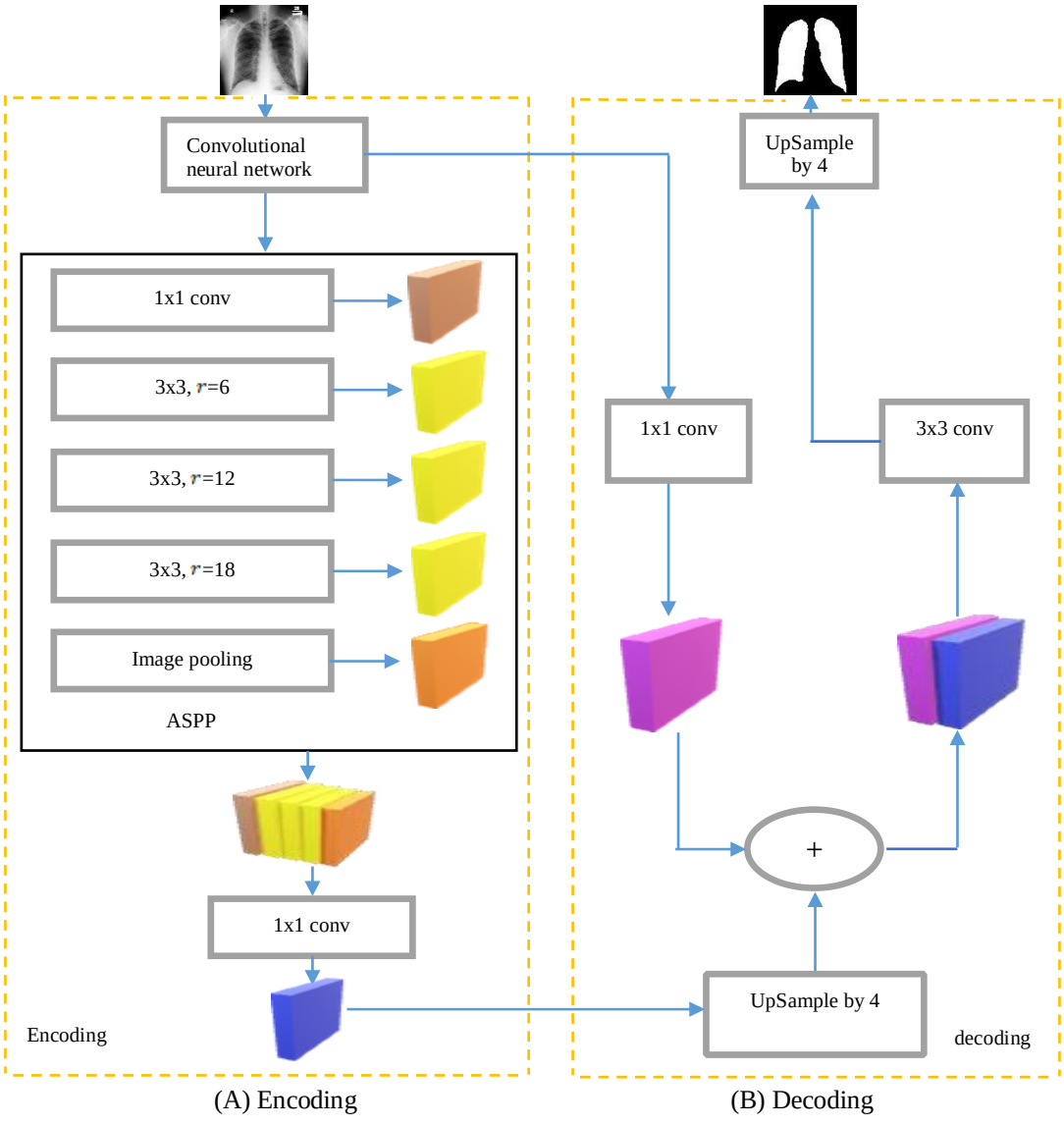

Figure 5. The encoder-decoder architecture

2.7. Dataset

In our project, we used the Montgomery County set - Chest X-ray Database, which is created by the National Library of Medicine, Maryland, the USA in collaboration with the Department of Health and Human Services. It's publicly available to use for many works. It contains 138 images (58 images for abnormal and 80 images for normal), the abnormal cases referred to the patient's diagnosed as affected by Tuberculosis disease. Images are in the image format (image-name.png image-type) with varies sizes, each image was named such as CHNCXR_####_0/1.png where the number 1 represents the normal cases and the number 0 represents the abnormal ones, it's also contained the ground truth masks for all images whereas each mask as same as the name of its properly image.

2.8. Pre-processes

Figure 6. Pre-processing

2.9. Post-process

After segmentation, we noted that few results have an unwanted object (dots) that must be removed, in these cases we used an operation called Area Opening which removes all components that have fewer pixels than the user-defined number of pixels [31][32].

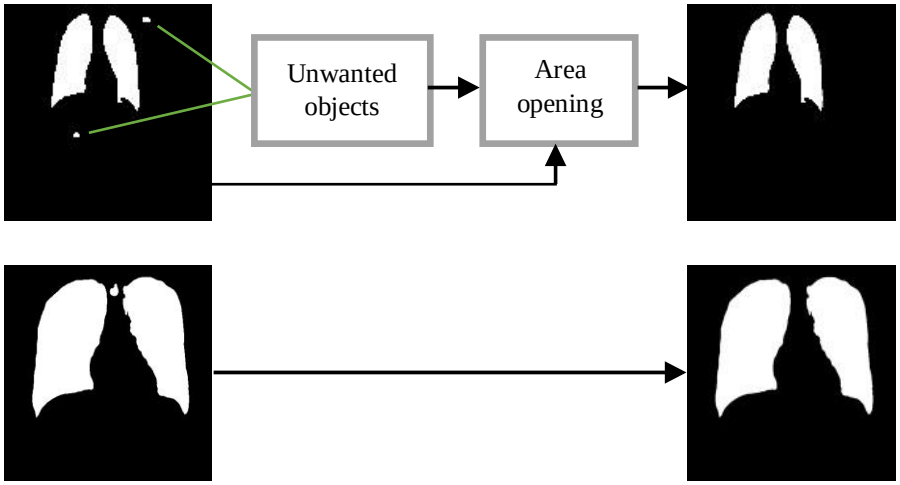

Figure 7. Resulted in mask before and after open area operation

4. Performance measurements

Let these symbols *TP, TN, FP, FN* represent true positives, true negatives, false positives, and false negatives, respectively. In semantic segmentation *TP* is referred to the number of foreground pixels that are correctly classified as foreground pixels, FP is referred to the number of pixels that are classified as foreground pixels but truly belongs to background pixels, *TN* is

referred to the number of background pixels which are classified as background pixels, *FN* is referred to the number of foreground pixels that are correctly classified as background pixels.

We used a lot of performance measurements to correctly evaluate the proposed system such that Accuracy, Dice, MCC, Jaccard, Sensitivity, Specificity, Precisionthen the measurement equations are:

$$Accuracy = \frac{TP+TN}{TP+TN+FP+FN} \tag{3}$$

$$Sensitivity = \frac{TP}{TP+FN} \tag{4}$$

$$Precision = \frac{TP}{TP+FP} \tag{5}$$

$$MCC \frac{(TP*TN-FP*FN)}{\sqrt{(TP+FP)*(TP+FN)*(TN+FP)*(TN+FN)}} \tag{6}$$

$$Dice = 2 * \frac{TP}{2*TP+FP+FN} \tag{7}$$

$$Jaccard = \frac{Dice}{2-Dice} \tag{8}$$

$$Specificity = \frac{TN}{TN+FP} \tag{9}$$

5. Experiments and result

To evaluate our model performance, we tested it on the Montgomery dataset, we used MATLAB 2020a to develop it with computer specifications such that Processor: Intel(R) Core (TM) i7-8750H CPU @ 2.20GHz (12 CPUs), ~2.2GHz, Memory: 16 GB of RAM and 4GB GeForce GTX 1050 ti.

We divided the dataset into two different subsets as 60% for training and the rest 40% for testing. We trained our model with sgdm optimizer, MiniBatchSize equals 4, initial base learning rate equals 0.0100, and a maximum number of epochs equals 30 epochs, then we compared our model with two other efficient models on the same dataset and same 60:40 ratio of data for training and testing phases, we repeated the experiment ten times, measurements are computed on average.

Table 1. The proposed model performance

Measurement	Performance
Accuracy	0.995002
Sensitivity	0.960642
Precision	0.979460
MCC	0.967081
Dice	0.969487
Jaccard	0.941546
Specificity	0.998189

Table 2. Comparison with other models

Paper	Dice	Jaccard	SEN	SPE	ACC
Proposed	0.969487	0.94154	0.96	0.998	0.995
[11]	0.954	N/A	0.954	0.985	0.977
[18]	0.960±0.018	0.941±0.034	N/A	N/A	N/A

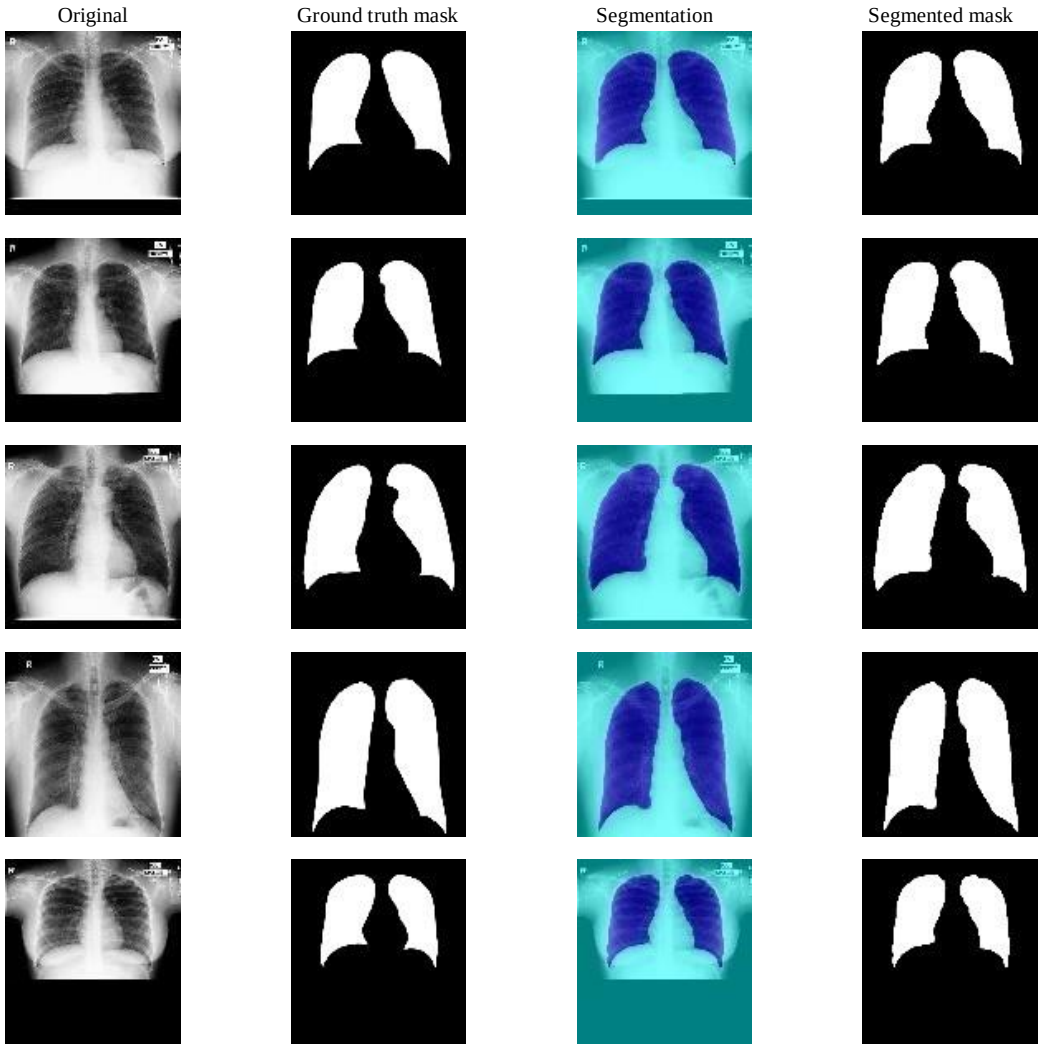

Figure 8. Sample results achieved by our model

According to the experimental results in [Figure 8], the proposed model detects and segments the area of a very promising pixel that almost be the entire area of the field which can be very clear when we look at the ground truth mask that had been drawn by the experts and the predicted mask by the proposed model which almost to be similar (successful segmentation). A problem we faced and successfully handled by the proposed model is that some outputs have irrelevant pixels (undesired) provided by the model which is covered by the opening area algorithm.

6. Conclusion

In this work, we proposed the DeepLabV3 with the ResNet-18 framework that is considered as an encoder and decoder architecture to provide a robust image semantic segmentation model that automatically segments the lung field from CHX-ray images. The encoding step is responsible for feature extraction by applying the ASPP convolution that is capable to capture very rich spatial information instead of the standard convolution. The decoding step is responsible for classifying the pixels into the foreground or background pixels. Our experiments show that this approach is very efficient, highly accurate, and very close to the expert's segmentation. This approach improves the state of the art of the neural networks and predicts very promising results and can be used for other tasks that need a very accurate semantic segmentation network to segment a specific area from the entire image. briefly encoding and decoding architectures are very powerful image semantic segmentation tools.

Reference

[1] V. Zazzu, B. Regierer, A. Kühn, R. Sudbrak, and H. Lehrach, "IT future of medicine: From molecular analysis to clinical diagnosis and improved treatment," N. Biotechnol., vol.30, no.4, pp.362-365, **(2013)**, DOI: 10.1016/j.nbt.2012.11.002

[2] J. Kalpathy-cramer, M. G. Hospital, and S. K. Antani, "Creating a classification of image types in the medical literature for visual categorization creating a classification of image types in the medical literature for visual categorization," no. February, **(2012)**, DOI: 10.1117/12.911186

[3] S. A. Naser and A. Mushtaha, "Knowledge management in ESMDA: Expert system for medical diagnostic assistance," vol.10, no.1, pp.31-40, **(2010)**

[4] M. I. Razzak, S. Naz, and A. Zaib, "Deep learning for medical image processing: Overview, challenges and the future," Lect. Notes Comput. Vis. Biomech., vol.26, pp.323-350, **(2018)**, DOI: 10.1007/978-3-319-65981-7_12

[5] D. Kaur and Y. Kaur, "Various image segmentation techniques: A review," Int. J. Comput. Sci. Mob. Comput., vol.3, no.5, pp.809-814, date accessed: 18/05/2016, 2014

[6] D. L. Pham, C. Xu, and J. L. Prince, "A survey of current methods in medical image segmentation," Annu. Rev. Biomed. Eng., **(2000)**

[7] R. Acharya, R. Wasserman, J. Stevens, and C. Hinojosa, "Biomedical imaging modalities: A tutorial," Comput. Med. Imaging Graph., vol.19, no.1, pp.3-25, **(1995)**, DOI: 10.1016/08956111(94)00043-3

[8] W. Dai et al., "SCAN: Structure correcting adversarial network for organ segmentation in chest x-rays,"

[9] X. Li, S. Luo, Q. Hu, J. Li, D. Wang, and F. Chiong, "Automatic lung field segmentation in x-ray radiographs using statistical shape and appearance models," J. Med. Imaging Heal. Informatics, vol.6, no.2, pp.338-348, 2016, DOI: 10.1166/jmihi.2016.1714

[10] S. Stirenko et al., "Chest x-ray analysis of tuberculosis by deep learning with segmentation and augmentation," 2018 IEEE 38th Int. Conf. Electron. Nanotechnology, ELNANO 2018 - Proc., pp.422-428, **(2018)**, DOI: 10.1109/ELNANO.2018.8477564

[11] R. Rashid, M. U. Akram, and T. Hassan, "Fully convolutional neural network for lungs segmentation from chest x-rays," Springer International Publishing, **(2018)**

[12] C. Wang, "Segmentation of multiple structures in chest radiographs using multi-task fully convolutional networks," Lect. Notes Comput. Sci. (including Subser. Lect. Notes Artif. Intell. Lect. Notes Bioinformatics), vol.10270 LNCS, December, pp.282-289, **(2017)**, DOI: 10.1007/978-3-319-59129-2_24

[13] M. Frid-Adar, A. Ben-Cohen, R. Amer, and H. Greenspan, "Improving the segmentation of anatomical structures in chest radiographs using U-net with an imagenet pre-trained encoder," Lect. Notes Comput. Sci. (including Subser. Lect. Notes Artif. Intell. Lect. Notes Bioinformatics), vol.11040 LNCS, pp.159-168, **(2018)**, DOI: 10.1007/978-3-030-00946-5_17

[14] Y. Tang, Y. Tang, J. Xiao, and R. M. Summers, "XLSor: A robust and accurate lung segmentor on chest," pp.1-11, **(2019)**

[15] R. Solovyev, I. Melekhov, T. Lesonen, E. Vaattovaara, O. Tervonen, and A. Tiulpin, "Bayesian feature pyramid networks for automatic multi-label segmentation of chest x-rays and assessment of cardio-thoracic ratio," Lect. Notes Comput. Sci. (including Subser. Lect. Notes Artif. Intell. Lect. Notes Bioinformatics), vol.12002 LNCS, pp.117-130, **(2020)**, DOI: 10.1007/978-3-030-40605-9_11

[16] W. Yang et al., "Lung field segmentation in chest radiographs from boundary maps by a structured edge detector," IEEE J. Biomed. Heal. Informatics, vol.22, no.3, pp.842-851, **(2018)**, DOI: 10.1109/JBHI.2017.2687939

[17] J. Xiong, Y. Shao, J. Ma, Y. Ren, Q. Wang, and J. Zhao, "Lung field segmentation using weighted sparse shape composition with robust initialization," Med. Phys., vol.44, no.11, pp.5916-5929, **(2017)**, DOI: 10.1002/mp.12561

[18] S. Candemir et al., "Lung segmentation in chest radiographs using anatomical atlases with nonrigid registration," IEEE Trans. Med. Imaging, vol.33, no.2, pp.577-590, **(2014)**, DOI: 10.1109/TMI.2013.2290491

[19] L. C. Chen, Y. Zhu, G. Papandreou, F. Schroff, and H. Adam, "Encoder-decoder with atrous separable convolution for semantic image segmentation," Lect. Notes Comput. Sci. (including Subser. Lect. Notes Artif. Intell. Lect. Notes Bioinformatics), vol.11211 LNCS, pp.833-851, **(2018)**, DOI: 10.1007/978-3-030-01234-2_49

[20] pac-20393494 @ www.mayoclinic.org.

[21] 38df733ae32e4c90ba37c7eb10f9f401dc90341e @ ecetutorials.com

[22] M. Yang, K. Yu, C. Zhang, Z. Li, and K. Yang, "DenseASPP for semantic segmentation in street scenes," Proc. IEEE Comput. Soc. Conf. Comput. Vis. Pattern Recognit., pp.3684-3692, **(2018)**, DOU: 10.1109/CVPR.2018.00388

[23] 5eb456147f2138c291e05b408c8ca7557ed5fbff @ developers.arcgis.com

[24] b20a114df970987b935f062faf603abda90fa71c @ machinelearningmastery.com

[25] G. Brain, G. Brain, and A. N. Gomez, "Depthwise separable convolutions for," Iclr, pp.1-10, **(2018)**

[26] upsampling-with-transposed-convolution-9ae4f2df52d0 @ medium.com

[27] b3b76e0887361b29dc0b1caf88d27d2d207a8540 @ machinelearningmastery.com

[28] Z. Zhang, X. Zhang, C. Peng, X. Xue, and J. Sun, "ExFuse: Enhancing feature fusion for semantic segmentation," Lect. Notes Comput. Sci. (including Subser. Lect. Notes Artif. Intell. Lect. Notes Bioinformatics), vol.11214 LNCS, pp.273-288, **(2018)**, DOI: 10.1007/978-3-03001249-6_17

[29] T. Wood, "Softmax-Layer @ Deepai.Org

[30] classificationlayer @ www.mathworks.com

[31] L. Vincent, "Morphological area openings and closings for grey-scale images," Shape Pict., pp.197-208, (1994), DOI: 10.1007/978-3-662-03039-4_13

[32] L. Vincent, "Grayscale area openings and closings: Their applications and efficient implementation," EURASIP Work. Math. Morphol. its Appl. to Signal Process., no. May, pp.22-27, (1993), [Online]. Available: http://www2.vincentnet.com/luc/papers/93barcelona_areaopen.pdf

Authors

Mohammed Ryiad Al-Eiadeh
Received the B.S. Degree in Computer Science from Al-Huston College from Al Balqa Applied University in summer 2018.
Currently, Mohammed is a Computer Science master's degree student in the Department of Computer Science at Al-Yarmouk University.